symmetry

MDPI

*Article*

# Rethinking Electron Statistics Rules

**Andras Kovacs [1,2,*] and Giorgio Vassallo [3]**

[1] BroadBit Energy Technologies, 02360 Espoo, Finland
[2] ExaFuse, Fletcher, NSW 2292, Australia
[3] Engineering Department, University of Palermo , 90128 Palermo, Italy; giorgio.vassallo@unipa.it
* Correspondence: andras.kovacs@broadbit.com

**Abstract:** The Fermi–Dirac and Bose–Einstein statistics are considered to be key concepts in quantum mechanics, and they are used to explain the occupancy limit of electron orbitals. We investigate the physical origin of these two statistics and uncover that the key determining factor is whether an individual electron spin is measurable or not. Microscopically, a system with individually measurable electron spins corresponds to the presence of Larmor spin precession in electron–electron interactions, while the non-measurability of individual electron spins corresponds to the absence of Larmor spin precession. Both interaction types are possible, and the favored interaction type is thermodynamically determined. The absence of Larmor spin precession is realized in coherent electron states, and coherent electrons therefore obey Bose–Einstein statistics.

**Keywords:** electron statistics; fermions; bosons; exclusion principle; spin correlation; electron coherence; Darwin Lagrangian

## 1. The Historic Origin of Electron Statistics Rules

Until the dawn of quantum mechanics, physics was irrelevant to chemistry. This situation changed dramatically with the introduction of quantum mechanics: the accurate calculation of electron binding energies has been quantum mechanics' main success, thus being able to clarify why fluorine takes an electron from lithium and not vice versa. This capability of binding energy calculations has eventually established quantum mechanics as a practical tool for the predictive modeling of chemical reactions.

However, the calculation of electron binding energies explains only half of chemistry; the remaining challenge 100 years ago was to explain the phenomenological observation that only two electrons can occupy any given atomic or molecular orbital. This electron occupancy limiting rule has become known as the exclusion principle.

**Phenomenological formulation of the exclusion principle, proposed by Pauli in the 1920s**: only one electron may occupy any quantum mechanical state, where the electron states are defined using four quantum numbers: principal quantum number ($n$), azimuthal quantum number ($l$), magnetic quantum number ($m$), and spin quantum number ($s$).

The above-formulated spin quantum number assignment was motivated by the observation of oppositely oriented spins of the electrons occupying an atomic orbital. When two electrons have different spin quantum numbers, they are said to be isotropically spin-correlated (ISC) into opposite directions: a spin measurement made in an *arbitrary* direction on *one* of the electrons allows us to predict with certainty the spin value of the *other* electron for the same direction. In other words, isotropic electron spin correlation is an observed precondition for the two-electron occupancy of a quantum mechanical orbital.

In each quantum mechanical state, the wavefunction forms a standing wave, and the state is characterized by a well-defined energy eigenstate. This energy eigenstate condition requires isotropic spin correlation among the electrons occupying a given state; otherwise, the apparent spin interaction energy would depend on the spin measurement direction, and there would not be a well-defined energy eigenstate. The presence of ISC electron

check for updates

**Citation:** Kovacs, A.; Vassallo, G. Rethinking Electron Statistics Rules. *Symmetry* **2024**, *16*, 1185. https://doi.org/10.3390/sym16091185

Academic Editor: Aurélien Drezet

Received: 5 August 2024
Revised: 25 August 2024
Accepted: 28 August 2024
Published: 10 September 2024

states thus follows from the energy eigenstate condition, and the challenge is to understand what limits the number of ISC electrons occupying a given quantum mechanical state.

Those quantum mechanical systems where the exclusion principle applies are said to obey Fermi–Dirac statistics, while quantum mechanical systems without the exclusion principle are said to obey Bose–Einstein statistics.

Aiming to derive the exclusion principle, Pauli proposed in the 1940s a spin-value-based distinction between Fermi–Dirac and Bose–Einstein statistics, but his arguments do not apply to spin-correlated particle pairs. The thousands of articles on the subject of "non-locality" attest that ISC states do not obey the principle of microcausality, which is at the core of Pauli's logic [1]. The exclusion principle has thus essentially remained in a postulate status.

## 2. Coherent versus Incoherent Electron States

Let us introduce the following classification of electron states:

- $N$ electrons are said to be in a **coherent** state if all quantum numbers of each electron are the same, i.e., they are all in the same quantum mechanical state.
- $N$ electrons are said to be in a **incoherent** state if each electron is in a different quantum mechanical state.

In a hypothetical coherent state, each involved electron is part of exactly the same quantum mechanical wave. In such a coherent state, individual electron properties may be measured only by such methods that resolve much shorter distances than the quantum mechanical wavelength; for example, the Compton scattering of radiation with a femtometer-scale wavelength still happens from individual electrons. But, any lower-resolution measurement on coherent electrons is a simultaneous measurement on all involved electrons.

In an incoherent state, each involved electron comprises a different quantum mechanical wave. In principle, it may be possible to measure individual electron properties by low-resolution measurements that resolve a longer-distance scale than the quantum mechanical wavelength.

In the following, we shall explore the applicable electron statistics for the above-defined incoherent versus coherent state classes.

## 3. Spin Correlations between Particles Occupying Different Orbitals

Isotropic spin correlation is observed not only for electrons sharing the same orbital but also for electrons in different orbitals. For example, the ground-state oxygen molecule is the so-called "triplet oxygen": it has two electrons occupying two distinct $\pi^*$ orbitals (anti-bonding orbital), and these two electrons are isotropically spin-correlated into parallel directions.

Isotropic spin correlation is observed between the nuclei comprising a molecule. For example, the hydrogen molecule has two nuclear spin isomers: the two protons of "ortho-hydrogen" are isotropically spin-correlated into parallel directions while the two protons of "para-hydrogen" are isotropically spin-correlated into opposite directions. This system is significant because the two nuclei are well separated in space; the individual spin state of each proton is thus measurable, in principle.

Isotropic spin correlation is observed between a bound electron and a nucleus: such an interaction generates the hyperfine split of the electron's binding energy. Isotropic spin correlation is also observed between a delocalized unpaired electron and a nucleus: such an electron–nucleus spin interaction shows up in NMR measurements, contributing to the Knight shift in metals.

In all observations, **ISC always occurs pair-wise**, i.e., the ISC of $N > 2$ particles is never observed. Table 1 illustrates this effect for the simplest atoms: an electron is either spin-correlated to an other electron or to a nucleus but never to both at the same time. Whether we look at particles sharing the same orbital or particles occupying different orbitals, we thus observe exactly the same phenomenology of strictly pair-wise ISC coupling.

This suggests the same origin of the ISC coupling limit, and we therefore look for a unifying principle. Taking the example of hydrogen spin isomers, it is obvious that Pauli's microcausality arguments do not apply to well-separated nuclei, and it is also obvious that there would be nothing anti-symmetric about the exchange of two separated nuclei.

**Table 1.** The pattern of spin correlations between electrons and the nucleus.

| | $p^+ + e^-$ **(H)** | $p^+ + 2e^-$ **($H^-$)** | $^3He^{2+} + e^-$ **($He^+$)** | $^3He^{2+} + 2e^-$ **(He)** |
|---|---|---|---|---|
| Hyperfine split | yes | no | yes | no |
| ISC electrons | - | yes | - | yes |

We approach the challenge of finding a unifying principle by firstly considering what spin measurement really means. It is well known by the operators of electron spin resonance (ESR) and nuclear magnetic resonance (NMR) equipment that the particle whose spin they measure is in a Larmor spin precession. Specifically, the magnetic moment vector generated by the particle's spin is Larmor precessing around the externally applied magnetic field lines. This Larmor spin precession's angular frequency is [2]

$$\omega_L = \frac{g\mu_B}{\hbar} B$$

where $B$ is the applied magnetic field strength, $\mu_B$ is the Bohr magneton, and $g \approx 1 + \frac{\alpha}{2\pi}$ is the gyromagnetic ratio of the electron spin. We note that the Larmor spin precession's frequency is half of the $\omega_{esr}$ "electron spin resonance" frequency [3]: $\omega_{esr} = 2\omega_L$. The $\omega_{esr}$ value is the experimentally measurable frequency of resonant flipping between the parallel and anti-parallel spin precession orientations with respect to a sinusoidally varying applied magnetic field. A consequence of the Larmor spin precession phenomenon is that the measured $\frac{\hbar}{2}$ spin angular moment, measured via an applied $B$ field, is only the component of the total angular momentum vector that is pointing along the applied $B$ field.

Is there a principal difference between the magnetic field applied by an external apparatus and the magnetic field applied by an external particle? Taking the example of a hydrogen molecule, the magnetic field applied onto the proton by another particle 74 pm away is principally not different from the magnetic field applied by an external apparatus. Taking the example of Knight shift measurements, the magnetic field applied onto the proton by a macroscopically delocalized electron wave is principally not different from the magnetic field applied by an external apparatus. It is clear from these examples that the magnetic field of one particle induces a Larmor spin precession of the other particle, i.e., each particle of the involved ISC pair undergoes Larmor spin precession. This concept is illustrated in Figure 1 for a hydrogen molecule's two protons: the two proton spins are aligned on the average, while their actual magnetic moment is in a precession. One may observe in Figure 1 interesting coupling dynamics for the $x$ component of the spin, where the $x$ axis connects the two protons. Taking the magnetic moment vector of the left proton to point toward the right proton, the right proton perceives a magnetic field pointing along the $x$ axis, and its magnetic moment vector will thus be in a precession around the $x$ axis. In turn, the left proton perceives a magnetic field coming at an angle with respect to the $x$ axis, causing a tilted precession cone that rotates in sync around the $x$ axis while the actual magnetic moment vector remains aligned with the $x$ axis. In essence, the entire magnetic field configuration depicted in Figure 1 is rotating around the $x$ axis. Similar coupling dynamics can be worked out for the $y$ and $z$ spin directions.

For the purpose of our analysis, we do not need to know details of spin precession dynamics because, in the following, we shall work with the time-averaged spin measurements of an ISC pair. The key point is the presence of Larmor spin precession and the individual measurability of particle spins.

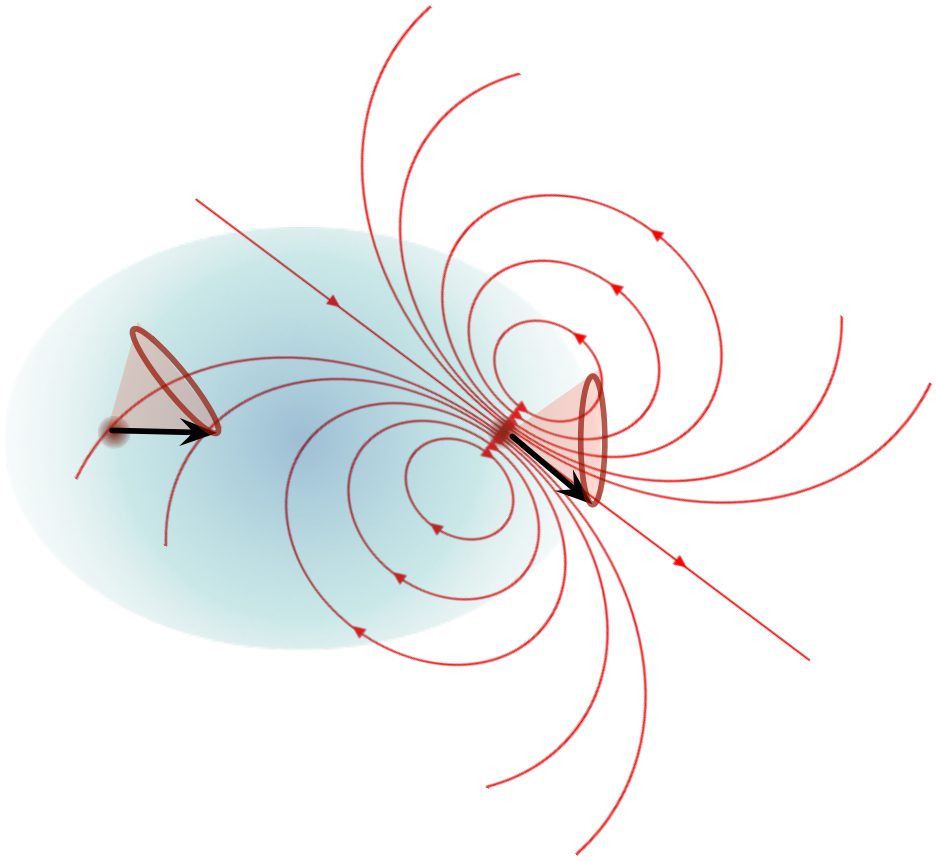

**Figure 1.** An illustration of two protons' Larmor spin precession in a hydrogen molecule. Each proton perceives the other proton's magnetic field (directed red curves) as an externally applied magnetic field and Larmor spin-precesses (cones with arrow) around the external magnetic field line.

We established through the above examples that the isotropic spin correlation of separated particles involves Larmor spin precession. At the same time, each involved particle has a principally measurable spin state, and thus we can investigate the origin of strictly $N = 2$ coupling by taking into account the fact of individually measurable spin states.

## 4. Isotropic Spin-Coupling Limit for Incoherent Electron States

Considering the phenomenologically observed pair-wise ISC coupling limit, regardless of the involved particles being on the same orbital or not, the question arises as to whether the two electrons sharing the same orbital might also be in Larmor spin precession with respect to the magnetic field generated by the other particle's spin. In the case of an antibonding molecular orbital, its two electrons have a large spatial separation distance because their wavefunction overlap region is mostly empty; therefore, these separated electrons again perceive the magnetic field of the other electron as an external field. In turn, this implies Larmor precession and an individually measurable spin state for two ISC electrons occupying an antibonding molecular orbital.

Let us finally consider an incoherent electron pair sharing the same bonding orbital: their wavefunctions overlap, and Zeeman split measurements yield the zero sum of the two oppositely oriented spins. Nevertheless, it may be possible to individually measure each electron's spin state by firstly separating them in such a way that does not disrupt their spin state and then measuring each electron's spin state. The principal feasibility of such an individual electron spin state measurement is demonstrated by reference [4], whose authors studied the molecular photo dissociation of $H_2$ and $D_2$ under linearly

polarized incident light, employing 33.66 eV photon energy. They measured the angular correlation function of electromagnetic Lyman-alpha radiation produced by the resulting atom pair in order to find out whether the atom pair is entangled or not. The authors of [4] conclude that an entangled electron pair is produced through the photo dissociation of a hydrogen molecule, and this entanglement originates from their molecular state. The results of [4] thus demonstrate that it is principally possible to photo-dissociate a bonding orbital occupying electron pair, without breaking their entanglement, and then measure their individual spin state.

Up to now, we have established that electrons occupying incoherent states can be always treated as electrons with individually measurable spin states. In the following, we consider the implications of individual spin measurability. By definition, $N$ electrons are said to be isotropically spin-correlated (ISC) if a measurement made in an *arbitrary* direction on *one* of the particles allows us to predict with certainty the spin value of each of the other $N-1$ particles for the same direction.

**Theorem 1.** *Incoherent ISC states exist only for* $N = 2$.

**Proof.** The idea of the following proof originates from Eugene Wigner, and it has been adapted by Paul O'Hara for proving the Pauli exclusion principle [5,6]. The logic of the following proof requires that each electron's spin state is individually measurable. For this reason, it only applies to incoherent states, where the electron wavefunctions are different.

Essentially, to show that ISC states exist only for $N = 2$, it is sufficient to prove that it is impossible to have three such particles. The impossibility of three ISC particles also excludes the possibility of $N \geq 3$ ISC particles.

Suppose that an ISC state exists for $N = 3$. We demonstrate in the following paragraphs that this assumption leads to a mathematical contradiction.

In the interest of clarity, assume without loss of generality that the three ISC particles are such that they are detected to be in $(+,+,+)$ correlation for an arbitrary measurement direction. Later, we will generalize the proof to any other correlation type. Define the $x$ axis along this arbitrary direction and define the $z$ axis in any orthogonal direction to $x$. We will perform further spin measurements in the $x-z$ plane. Spin measurements in orthogonal directions are statistically independent. Although we know a given particle spin to be $|+\rangle$ along the $x$ axis, a subsequent spin measurement along the $z$ axis of the apparatus gives a $\frac{1}{2}$ probability of measuring the $|-\rangle$ state. In general, a spin state in direction $2\theta$ with respect to the $x$ axis, given that it is in the state $|+\rangle$ with respect to the $x$ axis, can be constructed from the rotation $R$ and is given by $R|+\rangle = \cos\theta|+\rangle - \sin\theta|-\rangle$. Therefore, in direction $2\theta$, the probability of measuring the $|+\rangle$ state is $\cos^2\theta$ and that of measuring $|-\rangle$ is $\sin^2\theta$. Taking the $(x, 2\theta)$ direction with respect to two spin-correlated particles, the joint probabilities are $P(+,+) = \frac{1}{2}\cos^2\theta$ and $P(+,-) = \frac{1}{2}\sin^2\theta$. Similarly, for the ket $|-\rangle$, $R|-\rangle = \sin\theta|+\rangle + \cos\theta|-\rangle$ and the joint probabilities are $P(-,-) = \frac{1}{2}\cos^2\theta$ and $P(-,+) = \frac{1}{2}\sin^2\theta$. In principle, if three ISC particles exist, a sequence of spin-correlated measurements in the directions $2\theta_1,\ 2\theta_2,\ 2\theta_3$ can be performed on the three entangled particles. Let $(s_1(\theta_1), s_2(\theta_2), s_3(\theta_3))$ represent each particle's observed spin values in the three different directions. Recall that the above-stated spin correlation implies that if any particle is measured to be in the $s_i(\theta_i) = |+\rangle$ spin state, the probability of measuring another particle in the $s_j(\theta_j) = |-\rangle$ spin state becomes $\frac{1}{2}\sin^2(\theta_j - \theta_i)$.

Given that $s_n(\theta_n) = |\pm\rangle$ for each $n$, there exists only two possible values for each measurement, which we associate with "spin-up" and "spin-down", respectively. Hence, for three measurements, there are a total of eight possibilities. In particular,

$$\{(+,+,-),(+,-,-)\} \subset \{(+,+,-),(+,-,-),(-,+,-),(+,-,+)\}$$

implies the following probability relationship:

$$P\{(+,+,-),(+,-,-)\} \leq P\{(+,+,-),(+,-,-),(-,+,-),(+,-,+)\}$$

Consider the meaning of various subsets in the above inequality:

The $\{(+,+,-),(+,-,-)\}$ subset is interpreted as follows: we measured the spin of particle 1 to be in $|+\rangle$ state and particle 3 to be in $|-\rangle$ state. The corresponding probability is $\frac{1}{2}\sin^2(\theta_3-\theta_1)$.

The $\{(+,+,-),(-,+,-)\}$ subset is interpreted as follows: we measured the spin of particle 2 to be in $|+\rangle$ state and particle 3 to be in $|-\rangle$ state. The corresponding probability is $\frac{1}{2}\sin^2(\theta_3-\theta_2)$.

The $\{(+,-,-),(+,-,+)\}$ subset is interpreted as follows: we measured the spin of particle 1 to be in $|+\rangle$ state and particle 2 to be in $|-\rangle$ state. The corresponding probability is $\frac{1}{2}\sin^2(\theta_2-\theta_1)$.

Substituting the above terms into the above inequality, we arrive at

$$\frac{1}{2}\sin^2(\theta_3-\theta_1) \leq \frac{1}{2}\sin^2(\theta_3-\theta_2)+\frac{1}{2}\sin^2(\theta_2-\theta_1)$$

which is Eugene Wigner's interpretation of Bell's inequality. Taking $\theta_3-\theta_2=\theta_2-\theta_1=\frac{\pi}{6}$ and $\theta_3-\theta_1=\frac{\pi}{3}$ gives $\frac{1}{2}\geq\frac{3}{4}$, which is a contradiction. Therefore, three particles cannot all be in the same spin state with probability 1. □

We note that the specific value of electron spin plays no role in the proof of Theorem 1, which indicates the irrelevance of Pauli's spin-value-based classification.

The real reason behind the exclusion principle is the isotropic spin correlation requirement of eigenstate-occupying electrons, along with the impossibility of more than two such electrons in the case of individually measurable spins.

**Remark 1.** *The proof of the above theorem was worked out for $(+,+,+)$- or $(-,-,-)$-type spin correlation. To generalize the proof, suppose that the ISC particles are measured to be $(+,-,+)$ along an arbitrary measurement direction. Then, the spin outcomes in the three different directions $\theta_1$, $\theta_2$, $\theta_3$ can be written as*

$$\{(+,-,-),(+,+,-)\} \subset \{(+,-,-),(+,+,-),(-,-,-),(+,+,+)\}$$

*Essentially, this means that we flipped the $|+\rangle$ to $|-\rangle$ to represent the state of particle 2. Applying the same probability argument as before, but noting that $P\{(+,-,-),(-,-,-)\}=\frac{1}{2}\cos^2(\theta_3-\theta_2)$, the inequality becomes*

$$\frac{1}{2}\sin^2(\theta_3-\theta_1) \leq \frac{1}{2}\cos^2(\theta_3-\theta_2)+\frac{1}{2}\cos^2(\theta_2-\theta_1)$$

*Then, taking $\theta_3-\theta_2=\theta_2-\theta_1=\frac{\pi}{2}-\frac{\pi}{6}$ and $\theta_3-\theta_1=\pi-\frac{\pi}{3}$ gives, as before, $\frac{1}{2}\geq\frac{3}{4}$, which is a contradiction.*

## 5. Spin Statistics for Coherent Electron States

### *5.1. A Review of the Darwin Lagrangian*

In this section, we shall make use of the so-called Darwin Lagrangian, which we therefore briefly review. The Darwin Lagrangian is well known for modeling the interaction among a large number of massive charged particles. It is defined as follows:

$$\mathscr{L}_D = \sum_{a=1}^{N}\left\{\frac{1}{2}m_a v_a^2+\frac{1}{2}[e\boldsymbol{A}_a(\boldsymbol{r}_a)\cdot\boldsymbol{v}_a-e_a\phi_a(\boldsymbol{r}_a)]\right\} \tag{1}$$

where $\boldsymbol{r}_a$ is the vectorial position of a given particle, $e_a$ is its charge value, $\boldsymbol{v}_a$ is its velocity, and $m_a$ is its mass. $\boldsymbol{A}_a(\boldsymbol{r}_a)$ and $\phi(\boldsymbol{r}_a)$ are the vector potential and Coulomb potential at position $\boldsymbol{r}_a$, and $N$ is the total number of interacting particles.

The Coulomb potential $\phi_a(\boldsymbol{r}_a)$ is given by

$$\phi_a(\boldsymbol{r}_a) = \sum_{b \neq a}^{N} \frac{e_b}{r_{ab}}$$

where $r_{ab} = |\boldsymbol{r}_{ab}| = |\boldsymbol{r}_b - \boldsymbol{r}_a|$ is the Euclidean distance from other particles.

Particles $a$ and $b$ moving parallel to their distance vector have no magnetic interaction, and consequently only the $\boldsymbol{v}_{b\perp}$ component of the charge velocity vector shall contribute to the vector potential at $\boldsymbol{r}_a$:

$$\boldsymbol{v}_{b\perp} = \boldsymbol{v}_b - (\boldsymbol{v}_b \cdot \boldsymbol{r}_{uab})\boldsymbol{r}_{uab}$$

where $\boldsymbol{v}_b$ is the charge velocity vector, $\boldsymbol{v}_{b\perp}$ is its orthogonal component to the distance vector $\boldsymbol{r}_{ab}$, and $\boldsymbol{r}_{uab} = \frac{\boldsymbol{r}_{ab}}{r_{ab}}$ is the unit length vector.

The $\boldsymbol{A}_{ab}(\boldsymbol{r}_a)$ vector potential contribution of particle $b$ is therefore given by

$$\boldsymbol{A}_{ab}(\boldsymbol{r}_a) = \frac{e_b \boldsymbol{v}_{b\perp}}{r_{ab}} =$$

$$= \frac{e_b[\boldsymbol{v}_b - (\boldsymbol{v}_b \cdot \boldsymbol{r}_{uab})\boldsymbol{r}_{uab}]}{r_{ab}}$$

We note that $\boldsymbol{A}_{ba} \cdot \boldsymbol{v}_b = \boldsymbol{A}_{ab} \cdot \boldsymbol{v}_a$.

In the above equations, $\boldsymbol{A}_{ab}$ is the contribution of particle $b$ to the vector potential $\boldsymbol{A}_a$. The overall vector potential $\boldsymbol{A}_a$ at $\mathbf{r}_a$ is the sum of contributions by all other particles:

$$\boldsymbol{A}_a(\boldsymbol{r}_a) = \sum_{b \neq a}^{N} \boldsymbol{A}_{ab}(\boldsymbol{r}_a) = \sum_{b \neq a}^{N} \frac{e_b[\boldsymbol{v}_b - (\boldsymbol{v}_b \cdot \boldsymbol{r}_{uab})\boldsymbol{r}_{uab}]}{r_{ab}} \quad (2)$$

The $\boldsymbol{A}_a$ and $\phi_a$ terms are halved in the Darwin Lagrangian in order to avoid a double counting of contributions to the collective interaction potential, considering that $\boldsymbol{A}_{ab} \cdot \boldsymbol{v}_a = \boldsymbol{A}_{ba} \cdot \boldsymbol{v}_b$ and $\phi_{ab} = \phi_{ba}$.

### *5.2. A Brief Review of Electron Zitterbewegung*

The existence of electron Zitterbewegung was first suggested by De Broglie, who proposed the $mc^2/h$ oscillation frequency named after him, which was then directly described as a light-speed oscillation by Schrödinger. References [2,6] present an experimentally validated Zitterbewegung model of the electron structure. As shown in [2,6], the electron spin is generated by its circular Zitterbewegung oscillation. This idea of the electron spin being generated by circular Zitterbewegung oscillation has a long history; reference [7] presents a thorough discussion of this topic. The Thomson scattering phenomenon is electron–light interaction in the low-photon-frequency limit: it measures the electron's "reduced Compton radius" size, which corresponds to the radius of light-speed charge circulation at the $mc^2/h$ frequency.

We now demonstrate that the electron's quantum mechanical wavelength is in fact the Lorentz-transformed spatial component of its Zitterbewegung oscillation. Consider an electron moving at kinetic speed $v$. In relation to light-speed, its speed is characterized by $\beta = \frac{v}{c}$, $\gamma_L = \left(1 - \beta^2\right)^{-\frac{1}{2}}$ and rapidity $w$ defined as $\gamma_L = \cosh w$. It follows that $\cosh^2 w - \sinh^2 w = 1$, $\tanh w = \beta$, and $\sinh w = \gamma_L \beta$.

In the electron's rest frame, its Zitterbewegung is a time-wise oscillation. A relativistic boost rotates the time and space axes into each other according to the following hyperbolic rotation matrix:

$$\begin{pmatrix} ct' \\ x' \end{pmatrix} = \begin{pmatrix} \cosh w & -\sinh w \\ -\sinh w & \cosh w \end{pmatrix} \begin{pmatrix} ct \\ x \end{pmatrix}$$

Therefore, the time-wise Zitterbewegung oscillation of the rest frame acquires a spatial oscillation component in the boosted reference frame. Specifically, the Zitterbewegung frequency of the rest frame is $\frac{\omega}{2\pi} = \frac{m_0 c^2}{h}$, and this is commonly referred to as the De

Broglie frequency. The quantum mechanical wavenumber of the rest frame is $k_0 = 0$. The corresponding wavenumber in the boosted frame is

$$\frac{k}{2\pi} = \frac{\omega}{2\pi}\frac{\sinh w}{c} - k_0 \cosh w = \frac{\omega}{2\pi}\frac{\sinh w}{c}$$

Evaluating the right side of the above equation, we obtain

$$\frac{k}{2\pi} = \frac{m_0 c^2}{h}\frac{\gamma_L v}{c^2}$$

Rearranging the above equation, we finally obtain

$$\hbar k = (\gamma_L m_0)v = mv = p_{kinetic}$$

We recognize the above result as the basic postulate of quantum mechanics. However, it no longer needs to be a postulate: the appearing quantum mechanical wave is simply the Lorentz-transformed component of the electron's Zitterbewegung oscillation. In this sense, all quantum mechanical wavelength measurements validate the Zitterbewegung structure of the electron, with the Zitterbewegung frequency being $mc^2/h$.

By definition, a coherent state of electrons means that they maintain the same quantum mechanical wavelength; this implies the coherence of their Zitterbewegung phases, and vice versa.

### *5.3. The Stable Equilibrium of Coherent Electron States*

Considering the microscopic interaction among electrons, the Zitterbewegung Lagrangian of $N$ interacting charges can be written analogously to the Darwin Lagrangian, but replacing the kinetic electron speed with the light-speed Zitterbewegung speed vector $\boldsymbol{c}$. Specifically, the Zitterbewegung Lagrangian must include the contributions of all other charges:

$$\mathscr{L}_N = -\sum_{a=1}^{N}[e_a \boldsymbol{A}_a \cdot \boldsymbol{c}_a - e_a V_a] = 0 \tag{3}$$

where $\mathscr{L}_N = 0$ is the condition for stable equilibrium. In the above equation, $\boldsymbol{A}$ is the vector potential generated by electrons' Zitterbewegung rotation at light speed while $V$ is the Coulomb potential at their charge surface. In the following, we use $\boldsymbol{c}$ = 1 natural units notation for convenience. Calling $r_{ec}$ the electron charge radius, $r_e$ the Zitterbewegung radius, $m_e$ the electron mass, $\omega_e$ the Zitterbewegung angular speed, and $\boldsymbol{c}$ the charge velocity vector in a vacuum, we relate these values to each other in natural units notation:

$$V = \frac{e}{r_{ec}} = \frac{e}{\alpha r_e} = \frac{1}{e r_e}$$

$$\boldsymbol{A} = \frac{e\boldsymbol{c}}{\alpha r_e} = \frac{\boldsymbol{c}}{e r_e}$$

where $\alpha$ is the electromagnetic fine structure constant.

The relativistic momentum of the electron charge is always given by $e\boldsymbol{A}_a = m_a \boldsymbol{c}_a$. Calling $m_o$ the electron rest mass, the kinetic energy term of any given electron can be written as

$$e\boldsymbol{A}_a \cdot \boldsymbol{c}_a = m_a \boldsymbol{c}_a \cdot \boldsymbol{c}_a = m_a = \gamma m_0 = \frac{m_0}{\sqrt{1 - v_a^2}} \simeq m_0 + \frac{1}{2} m_0 v_a^2 \tag{4}$$

The above result means that the $e_a \boldsymbol{A}_a \cdot \boldsymbol{c}_a$ term already incorporates the electron kinetic energy. Equation (3) therefore gives the complete Lagrangian equation: unlike in the classical Darwin Lagrangian case, there is no additional $\frac{1}{2} m_a v_a^2$ term.

Using $\mathscr{L}_N = 0$ as the condition for a stable equilibrium, we shall demonstrate the existence of a coherent state of $N$ electrons as a stable equilibrium state.

**Theorem 2.** *In the absence of noise, N coherent electrons may form a stable equilibrium state.*

**Proof.** When $N = 1$, the Lagrangian expression becomes $\mathscr{L}_a = -[e_a \boldsymbol{A}_a \cdot \boldsymbol{c}_a - e_a V_a]$. $\mathscr{L}_a$ is always zero as a consequence of the two Aharonov–Bohm equations that relate the Zitterbewegung rotation phase $\varphi$ to the electromagnetic potentials. To see this, let us calculate the differential $d\varphi$ term, keeping in mind that the Zitterbewegung phase is equivalent to the quantum mechanical wavefunction's phase.

On the one hand, the $d\varphi$ phase change can be calculated from the magnetic Aharonov–Bohm equation:

$$d\varphi = e_a \boldsymbol{A}_a \cdot \boldsymbol{dl} = e_a \boldsymbol{A}_a \cdot \boldsymbol{c_a} dt$$

On the other hand, the same $d\varphi$ phase change can be calculated from the electric Aharonov–Bohm equation:

$$d\varphi = e_a V_a dt$$

Dividing the above two equations by $dt$, we can equate them. Consequently,

$$\mathscr{L}_a = -[e_a \boldsymbol{A}_a \cdot \boldsymbol{c}_a - e_a V_a] = 0 \tag{5}$$

$$e_a \boldsymbol{A}_a \cdot \boldsymbol{c}_a = e_a V_a$$

The above result means that each individual electron's total energy is the same as the potential energy on the surface of its electric charge.

We now evaluate $\boldsymbol{A}_a(\boldsymbol{r}_a)$ and $V_a(\boldsymbol{r}_a)$ for $N$ interacting electrons:

$$\boldsymbol{A}_a(\boldsymbol{r}_a) = \frac{e_a \boldsymbol{c}_a}{\alpha r_{ea}} + \frac{1}{2} \sum_{i \neq j} \frac{e_b \boldsymbol{c}_{b\perp}}{r_{ab}} = \tag{6}$$

$$= \frac{e_a \boldsymbol{c}_a}{\alpha r_{ea}} + \frac{1}{2} \sum_{a \neq b} \frac{e_b [\boldsymbol{c}_b - (\boldsymbol{c}_b \cdot \boldsymbol{r}_{uab}) \boldsymbol{r}_{uab}]}{r_{ab}}$$

$$V_a(\boldsymbol{r}_a) = \frac{e_a}{\alpha r_{ea}} + \frac{1}{2} \sum_{a \neq b} \frac{e_b}{r_{ab}} \tag{7}$$

In both of these last two equations, the first terms are the self-interaction contributions. In Equation (6), the $\boldsymbol{c}_{b\perp}$ component of the charge velocity vector $\boldsymbol{c}_b$ is orthogonal to the distance vector $\boldsymbol{r}_{ab}$. Analogously to the Darwin Lagrangian case, only this $\boldsymbol{c}_{b\perp}$ component will contribute to the value of the vector potential $\boldsymbol{A}_a(\boldsymbol{r}_a)$.

The $e_a \boldsymbol{A}_a \cdot \boldsymbol{c}_a$ and $e_a V_a$ terms of Equation (3) can now be calculated as follows:

$$e_a \boldsymbol{A}_a \cdot \boldsymbol{c}_a = \frac{e_a^2}{\alpha r_{ea}} \boldsymbol{c}_a^2 + \frac{1}{2} \sum_{a \neq b} \frac{e_a e_b [\boldsymbol{c}_b - (\boldsymbol{c}_b \cdot \boldsymbol{r}_{uab}) \boldsymbol{r}_{uab}] \cdot \boldsymbol{c}_a}{r_{ab}}$$

$$e_a V_a = \frac{e_a^2}{\alpha r_{ea}} + \frac{1}{2} \sum_{a \neq b} \frac{e_a e_b}{r_{ab}}$$

where $e_a^2 = \alpha$ and $\boldsymbol{c}_a^2 = 1$.

Since all charged particles are electrons, it is possible to write their charges as $e_a e_b = \alpha$, and the expression for $\mathscr{L}_N$ becomes

$$\mathscr{L}_N = -\sum_{a=1}^{N}\left[\frac{e_a^2}{\alpha r_{ea}}\boldsymbol{c}_a^2 - \frac{e_a^2}{\alpha r_{ea}} + \frac{1}{2}\sum_{a\neq b}\frac{\alpha[\boldsymbol{c}_a\cdot\boldsymbol{c}_b - (\boldsymbol{c}_a\cdot\boldsymbol{r}_{uab})(\boldsymbol{c}_b\cdot\boldsymbol{r}_{uab}) - 1]}{r_{ab}}\right] \tag{8}$$

Considering that the charge speed is always $c = 1$, the first two terms of the above expression cancel out. Equation (8) therefore simplifies to

$$\mathscr{L}_N = -\frac{1}{2}\sum_{a=1}^{N}\sum_{a\neq b}\frac{\alpha[\boldsymbol{c}_a\cdot\boldsymbol{c}_b - (\boldsymbol{c}_a\cdot\boldsymbol{r}_{uab})(\boldsymbol{c}_b\cdot\boldsymbol{r}_{uab}) - 1]}{r_{ab}}$$

This $\mathscr{L}_N$ Lagrangian is zero (i.e., minimized) for a collection of coherent electrons where the Zitterbewegung phase is the same for all electron charges, and their Zitterbewegung planes are parallel to each other. In this case, $\boldsymbol{c}_a\cdot\boldsymbol{c}_b = 1$, and $\boldsymbol{c}_a\cdot\boldsymbol{r}_{uab} = \boldsymbol{c}_b\cdot\boldsymbol{r}_{uab} = 0$. The $\mathscr{L}_N = 0$ result directly follows from these conditions, and therefore the phase-coherent state of electrons is a stable equilibrium state. The proof of Theorem 2 is thus complete. □

Figure 2 illustrates this microscopic constellation of coherent electrons. We emphasize that the position of coherent electrons is stable only with respect to each other but remains undetermined with respect to the laboratory frame: each delocalized electron forms a standing wave, and their positions are distributed within the standing wave. While Figure 2 illustrates a single direction of motion, bound electron states involve a superposition of this picture along all three spatial axes. This point is demonstrated by the derivation of the Schrödinger equation in reference [8], which starts from the Lagrangian given by Equation (5).

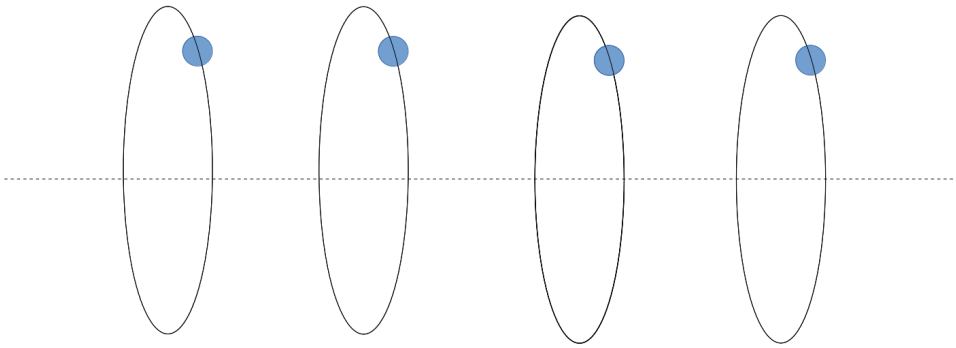

**Figure 2.** An illustration of electrons' coherent state. The dotted line represents the shared Zitterbewegung axis, the ellipses represent the 0.386 pm radius Zitterbewegung trajectories, and the blue spheres represent the electron charges. Each electron has the same momentum, and their kinetic speed vectors point along the Zitterbewegung axis.

The above results directly show the absence of Larmor spin precession in coherent electrons' equilibrium planes; the involved Zitterbewegung planes remain parallel to each other. Since all coherent electrons are part of the exact same quantum mechanical wave, individual electron spin measurement is impossible. The $\mathscr{L}_N = 0$ condition of Equation (8) allows for adding any number of electrons, and therefore we conclude that **coherent electrons obey Bose–Einstein statistics.**

Recalling that any electron's momentum is given by $e_a\boldsymbol{A}_a$, we can write down the Hamiltonian that corresponds to $\mathscr{L}_N$:

$$\mathscr{H}_N = \left[\sum_{a=1}^{N} e_a\boldsymbol{A}_a\cdot\boldsymbol{c}_a\right] - \mathscr{L}_N = \sum_{a=1}^{N} e_a\boldsymbol{A}_a\cdot\boldsymbol{c}_a - [e_a\boldsymbol{A}_a\cdot\boldsymbol{c}_a - e_aV_a] \tag{9}$$

$$\mathscr{H}_N = \sum_{a=1}^{N} e_a V_a$$

where we use Equation (3) for evaluating $\mathscr{L}_N$.

The obtained Hamiltonian expression is rather simple. According to Equation (7), $V_a$ is minimized when the coherent electrons are as far apart as possible. The various constellations of inter-electron distances can be understood analogously to atomic orbitals: all atomic orbitals are equilibrium states, and the ground-state orbital is the energy-minimizing equilibrium state. Therefore, in the energy-minimizing coherent state, $N$ electrons maximize their distance—within the constraints of their enclosure.

One may also calculate the action function corresponding to $\mathscr{L}_N$: this calculation can be found in reference [8] for the $N = 1$ case, and it shows that the action function corresponds to the Schrödinger equation.

## 6. Is Superconductivity the Realization of Coherent Electron States?

### *6.1. The Bose-Einstein condensed state of superconducting electrons*

A superconductor is defined by its ability to conduct electric current without any measurable resistance below a certain critical temperature ($T_c$). Since electric resistivity originates from scattering on crystal defect sites, superconducting electrons must have the ability to pass through the superconducting material without any scattering on such defect sites. The simplest way to achieve such an effect is to add and remove those conduction-band electrons whose wavefunction has a macroscopically large wavelength. Such a large wavelength no longer scatters on defect sites because of the many orders of magnitude mismatch with respect to the inter-nuclear distance. This simplest model naturally suggests some delocalized electrons' Bose–Einstein condensation, which then accumulate in the lowest-lying delocalized states.

Despite the above outlined natural match between superconductivity phenomena and Bose–Einstein condensation, and despite overwhelming experimental evidence of some form of electron coherence, superconductivity theorists refused to consider Bose–Einstein condensation-based models in the past. Historically, theorists have focused on constructing a phenomenological Hamiltonian, which has become known as the BCS theory of superconductivity. This BCS Hamiltonian was initially formulated over 60 years ago. The author of [9] emphasizes that BCS theory is phenomenological, and as such it does not yet provide any physical explanation: "We have all been taught that it [the BCS theory] is a marvellous success of quantum theory, accounting for persistent currents, Meissner effect, isotope effect, Josephson effect, etc. Yet on examination one realizes that the model Hamiltonian is phenomenological, chosen not from first principles but from trial-and-error so as to agree with just those experiments. Then in what sense can one claim that the BCS theory gives a *physical explanation* of superconductivity? Surely, if the Meissner effect did not exist, a different phenomenological model would have been invented, that does not predict it; one could have claimed just as great a success for quantum theory whatever the phenomenology to be explained". This phenomenological BCS theory's critical review can be found in [10].

At present, the Bose–Einstein-condensed state of superconducting electrons is receiving gradual recognition as a proper physical explanation of superconductivity phenomena [11,12]. In particular, reference [12] presents an experimentally matching superconductivity model via a thermodynamic analysis of Bose–Einstein condensates.

The key relevance of spin interactions to superconductivity has been recognized by the authors of references [11,13]. As can be seen in Figure 3, a correlation between the superconducting temperature $T_c$ and spin fluctuation temperature $T_{SF}$ is established over a very wide temperature range and across various superconductor families. The correlation depicted in Figure 3 is called the Moriya–Ueda law. The $T_{SF}$ parameter is derived from the frequency spread of spin fluctuations. Reaching a high superconducting temperature thus requires a very dynamic re-organization of electron spin correlations.

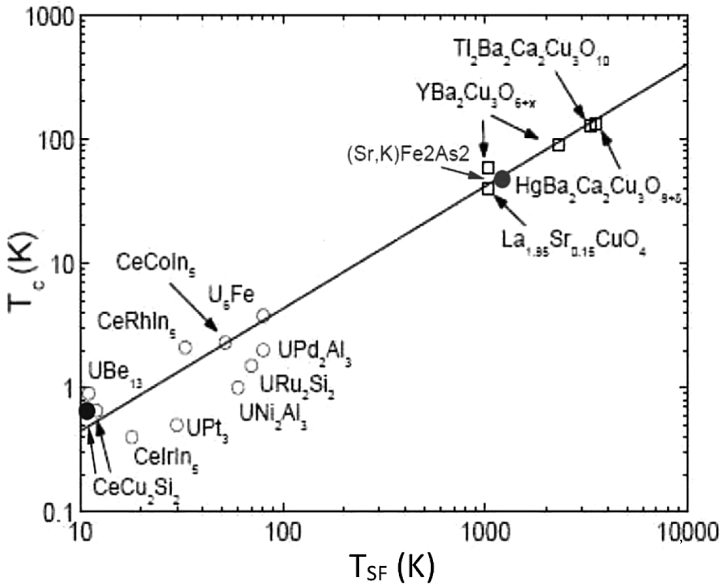


**Figure 3.** The correlation between $T_c$ and spin fluctuation temperature $T_{SF}$ in various superconductors. Reproduced from [11].

### *6.2. Preceding Meissner Effect Models*

The key role of electron coherence in superconductivity can be demonstrated via the analysis of superconductors' perfect diamagnetism, i.e., the Meissner effect. In the following paragraphs, we discuss the Meissner effect in the context of BCS theory versus our theory. While both approaches propose bosonic states of coherent electrons, the Meissner effect explanations become radically different.

The BCS theory of superconductivity is described in reference [14]; this publication won the Nobel prize for its authors. According to BCS theory, only short-wavelength electrons near the Fermi surface have a coherent wavefunction. The authors of reference [14] calculate the existence of a persistent diamagnetic current around the superconducting perimeter and describe the Meissner effect as the consequence of this persistent current circulation. As the temperature is lowered from just above $T_c$ to just below $T_c$ while the superconductor is in a magnetic field, BCS theory claims that the appearance of bound electron–phonon states causes an electromotive force that induces Meissner current circulation. The main drawback of BCS theory is that circulating electrons have radial acceleration, and therefore must radiate energy. This means that the Meissner effect must either diminish with time or, otherwise, it must constantly draw energy from phonons, thereby cooling the material. Both of these possibilities are contradicted by experiments, and the implied "superconducting synchrotron radiation" also remains undetected. To remedy this issue, BCS theorists proposed that superconducting electrons' electromagnetic interactions are governed by a modified Maxwell's equation, while all other electrons interact via the ordinary Maxwell equation. Specifically, BCS theory proposes the presence of a phonon-related "Goldstone field" that interacts only with superconducting electrons and causes their electromagnetic interactions to become short-range, thereby preventing circulating electrons from emitting radiation. In other words, longitudinal phonons supposedly oscillate in precisely such a way that extinguishes the radiation that would otherwise be emitted by circulating superconducting electrons. Besides lacking any supporting experimental evidence, this Goldstone field model is also contradicted by the work of Pierre-Gilles de Gennes, who proposed that the Meissner effect minimizes the total energy of the system, where the magnetic energy density is given by the usual $\frac{1}{2\mu_0}\boldsymbol{B}^2$ expression, without any modifications [15].

*6.3. The London Equation*

In contrast to the above-outlined complex theories, we employ simple thermodynamic considerations. Bose–Einstein-condensed electrons start accumulating at the longest wavelengths, where the energy gain of multi-electron state occupancy is the highest. Let us consider what the thermodynamic equilibrium looks like in a superconducting material, immersed in an external magnetic field. Perfect diamagnetism means that the magnetic energy density is zero in the interior. In contrast, there is magnetic energy density $\varrho_m$ in the exterior, while superconducting electrons' translational kinetic energy density $\varrho_k$ is zero in that region. The challenge is to understand what happens in the transitional surface region between the exterior and interior zones, where $\varrho_m$ and $\varrho_k$ are both non-zero.

Anywhere in the surface region, magnetic energy density is given by

$$\varrho_m = \frac{1}{2\mu_0}\boldsymbol{B}^2 \tag{10}$$

The kinetic energy density of superconducting electrons is

$$\varrho_k = \frac{m_{eff}}{2}\boldsymbol{v}_s^2 n_s \tag{11}$$

where $n_s$ is the density of superconducting electrons, $m_{eff}$ is their effective mass, and $\boldsymbol{v}_s$ is their velocity. The corresponding current can be written as

$$\boldsymbol{J} = e\boldsymbol{v}_s n_s$$

Maxwell's equation defines the relationship between $\boldsymbol{J}$ and $\boldsymbol{B}$:

$$\mu_0 \boldsymbol{J} = \nabla \times \boldsymbol{B}$$

Substituting the above two equations into (11), we express kinetic energy density in terms of magnetic field:

$$\varrho_k = \frac{m_{eff}}{2e^2\mu_0^2 n_s}(\nabla \times \boldsymbol{B})^2 \tag{12}$$

Using Equations (10) and (12), we can express the total energy density as a function of magnetic field:

$$\varrho(\boldsymbol{B}) = \varrho_m + \varrho_k = \frac{1}{2\mu_0}\boldsymbol{B}^2 + \frac{m_{eff}}{2e^2\mu_0^2 n_s}(\nabla \times \boldsymbol{B})^2 \tag{13}$$

**Theorem 3.** *The magnetic field configuration of a superconducting surface region minimizes the total energy of the system.*

**Proof.** The following proof originates from the idea of Pierre-Gilles de Gennes, who proposed that the London equation describes the energy-minimizing magnetic field configuration, but without proving this proposition [15]. As far as the authors know, all citations of de Gennes' work just replicate this proposition, but always without proof. Our proof therefore represents the first mathematically complete derivation of the London equation. Suppose that there is a disturbance of or variation in the stationary magnetic field; we denote this magnetic field variation as vector field $\boldsymbol{G}$. The derivative of energy density with respect to infinitesimal magnetic field variations is

$$\varrho'(\boldsymbol{B}, \boldsymbol{G}) = \frac{\partial}{\partial \varepsilon}\varrho(\boldsymbol{B} + \varepsilon \boldsymbol{G}) \mid_{\varepsilon \to 0} \tag{14}$$

We now evaluate the above differential by substituting Equation (13):

$$\varrho'(\boldsymbol{B}, \boldsymbol{G}) = \frac{1}{\mu_0}(\boldsymbol{B} \cdot \boldsymbol{G}) + \frac{m_{eff}}{e^2\mu_0^2 n_s}(\nabla \times \boldsymbol{B}) \cdot (\nabla \times \boldsymbol{G}) \tag{15}$$

where we obtained the last term by switching the order of the two differential operators:

$$\frac{\partial}{\partial \varepsilon}(\nabla \times (\boldsymbol{B} + \varepsilon \boldsymbol{G})) = \nabla \times \frac{\partial}{\partial \varepsilon}(\boldsymbol{B} + \varepsilon \boldsymbol{G}) = \nabla \times \boldsymbol{G}$$

The thermodynamic equilibrium requires that the total system energy remains invariant with respect to small changes in the magnetic field, i.e., the system occupies the lowest energy state:

$$\int_{\Omega} \varrho'(\boldsymbol{B}, \boldsymbol{G})\, dV = 0$$

for any choice of $\boldsymbol{G}$, keeping in mind that the variational field $\boldsymbol{G}$ vanishes at the boundary. The above equilibrium requirement also guarantees that the superconducting-to-normal phase transition is reversible, which is compatible with calorimetric measurements. Substituting Equation (15) into the above equilibrium requirement, we obtain

$$\int_{\Omega} \left[ \frac{1}{\mu_0}(\boldsymbol{B} \cdot \boldsymbol{G}) + \frac{m_{eff}}{e^2 \mu_0^2 n_s}(\nabla \times \boldsymbol{B}) \cdot (\nabla \times \boldsymbol{G}) \right] dV = 0$$

We use the $\int_{\Omega}(\nabla \times \boldsymbol{B}) \cdot (\nabla \times \boldsymbol{G})\, dV = \int_{\Omega}(\nabla \times (\nabla \times \boldsymbol{B})) \cdot \boldsymbol{G}\, dV$ identity, which is proven in Appendix A. Note that we substituted $\nabla \times \boldsymbol{B}$ for the vector field $\boldsymbol{F}$ that is used in Appendix A. The above equation can therefore be written as

$$\int_{\Omega} \left[ \frac{1}{\mu_0}\boldsymbol{B} + \frac{m_{eff}}{e^2 \mu_0^2 n_s} \nabla \times (\nabla \times \boldsymbol{B}) \right] \cdot \boldsymbol{G}\, dV = 0$$

Since the above equation must remain zero for any choice of $\boldsymbol{G}$, the equilibrium condition is given by

$$\boldsymbol{B} + \frac{m_{eff}}{\mu_0 n_s e^2} \nabla \times (\nabla \times \boldsymbol{B}) = 0 \tag{16}$$

which is known as the London equation. Our simple derivation shows that the London equation solves for the lowest energy state. □

Since magnetic fields have zero divergence, we obtain $\nabla \times (\nabla \times \boldsymbol{B}) = -\nabla^2 \boldsymbol{B}$, and the London equation may be written as

$$\nabla^2 \boldsymbol{B} = \frac{\mu_0 n_s e^2}{m_{eff}} \boldsymbol{B} \tag{17}$$

The solution of the above equation is a $\boldsymbol{B} = \boldsymbol{B}_0 e^{-x/\lambda_L}$-type exponential decay of $\boldsymbol{B}$ from the surface toward the interior, over the characteristic distance $\lambda_L$:

$$\frac{1}{\lambda_L} = \sqrt{n_s \frac{\mu_0 e^2}{m_{eff}}} \tag{18}$$

### *6.4. The Microscopic Structure of Meissner Flows*

The above derivation of the London equation is generically formulated, and one may ask why it does not apply to ordinary metals. The traditional answer has been that $\varrho_k$ represents a translational motion that loses energy in ordinary metals but does not lose energy in superconductors. However, such an answer is wrong because it leads to the above-discussed paradox of missing synchrotron radiation. Consequently, $\varrho_k$ must represent microscopic circular flows; these flows correspond to some quantum mechanical ground state that cannot lose kinetic energy via radiation. Figure 4 illustrates this microscopic Meissner flow structure. In ordinary metals, the incoherent Fermi sea wavefunctions

comprise standing wave modes; these standing waves do not have any degree of freedom for a microscopic oscillation as shown in Figure 4.

As discussed at the end of Section 5, coherent electron states are occupied by a large number of electrons, and their inter-electron distances may vary while maintaining their coherent state. This opens up a new degree of freedom for microscopic oscillations: the density of coherent electrons can fluctuate around positively charged nuclei.

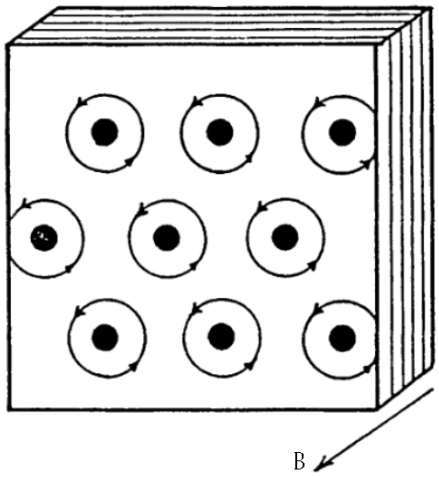


**Figure 4.** An illustration of vortices that comprise the Meissner flow. The externally applied magnetic field (B) is represented by the arrow.

Finally, we may calculate the radius of Meissner flow vortices. A microscopic circular flow can be modeled as a density oscillation of coherent electrons in the $x$ and $y$ directions, with a $\frac{\pi}{2}$ phase between them. The electron density oscillation around fixed positive charges is a so-called Langmuir oscillation, and its angular frequency $\omega_L$ is derived as follows. Suppose that the density of superconducting electrons has a variation $\delta n_s$ from the mean, and the average flow speed of these electrons is $v$. The continuity condition along the $x$ direction becomes

$$\frac{\partial(\delta n_s)}{\partial t} = -n_s \frac{\partial v}{\partial x} \tag{19}$$

Taking the time differential of the above equation, we obtain

$$\frac{\partial^2(\delta n_s)}{\partial t^2} = -n_s \frac{\partial}{\partial t}\frac{\partial v}{\partial x} = -n_s \frac{\partial}{\partial x}\frac{\partial v}{\partial t} \tag{20}$$

The electron density variation $\delta n_s$ generates an electric field $E$ according to Poisson's equation:

$$\frac{\partial E}{\partial x} = -\frac{e}{\varepsilon_0}\delta n_s \tag{21}$$

The generated $E$ field changes the momentum of superconducting electrons:

$$m_{eff}\frac{\partial v}{\partial t} = -eE \tag{22}$$

where $m_{eff}$ is the effective electron mass. Substituting Equations (21) and (22) into (20), we obtain a wave equation for $\delta n_s$:

$$\frac{\partial^2(\delta n_s)}{\partial t^2} = \frac{e n_s}{m_{eff}}\frac{\partial E}{\partial x} = -\frac{e^2 n_s}{\varepsilon_0 m_{eff}}\delta n_s \tag{23}$$

This wave equation is solved by the oscillatory motion of superconducting electrons at the following angular frequency:

$$\omega_L = \sqrt{\frac{e^2 n_s}{\varepsilon_0 m_{eff}}}$$

An analogous analysis for the $y$ direction yields the same frequency. This angular frequency $\omega_L$ is the natural oscillation frequency of superconducting electrons. We notice that $\omega_L$ can be expressed in terms of the London penetration depth parameter, which is given by Equation (18):

$$\omega_L = \sqrt{c^2}\sqrt{n_s \frac{\mu_0 e^2}{m_{eff}}} = \frac{c}{\lambda_L} \tag{24}$$

This remarkable relationship demonstrates that $\varrho_k$ corresponds to superconducting electrons' Langmuir oscillation. Such oscillations in the $x$ and $y$ directions result in a vortex motion of superconducting electrons, which generates their diamagnetic response. Since this vortex is in a quantum mechanical ground state, the involved angular momentum is quantized to $\hbar$:

$$m_{eff} r_{\circlearrowleft} (r_{\circlearrowleft} \omega_L) = \hbar \tag{25}$$

where $r_{\circlearrowleft}$ is the Meissner vortex radius illustrated in Figure 4. We can now solve for $r_{\circlearrowleft}$:

$$r_{\circlearrowleft} = \sqrt{\frac{\hbar}{m_{eff}\omega_L}} = \sqrt{\frac{\hbar \lambda_L}{m_{eff} c}} \tag{26}$$

Using the above result, one may evaluate $r_{\circlearrowleft}$ for various superconducting materials. As $\lambda_L$ grows with increasing temperature, $r_{\circlearrowleft}$ also grows along.

To validate the Langmuir oscillation model of Meissner vortices, we evaluate $r_{\circlearrowleft}$ for two well-known superconductors. The lead material has $\lambda_L(T \to 0)$ = 52 nm and $m_{eff} = 1.9 m_e$ parameters, yielding $r_{\circlearrowleft}$ = 0.1 nm at low temperatures. The $YBa_2Cu_3O_{6.95}$ material, which is a representative high-temperature superconductor, has $\lambda_L(T \to 0)$ = 140 nm and $m_{eff} \approx 2.2 m_e$ parameters, yielding $r_{\circlearrowleft}$ = 0.16 nm at low temperatures. At low temperatures, the $2r_{\circlearrowleft}$ diameter has a similar size to the unit cell dimension of these materials. These examples demonstrate that, at $T \to 0$, a Meissner vortex has a similar diameter to the unit cell size. This makes sense because these microscopic Langmuir oscillations are centered around the positively charged Pb and Cu sites, respectively, for these materials.

In summary, the superconducting state of electrons therefore appears to be a practical realization of the coherent-state analysis presented in Section 5. The noise-limited nature of coherent electron states is evidenced by the low critical temperature of most superconductors.

## 7. Discussion

Our results demonstrate that it is the presence or absence of Larmor spin precession in electron–electron interactions that determines the applicable statistics. A stable quantum mechanical wavefunction is an eigenstate solution of the Dirac equation, and such an eigenstate requires isotropic spin correlation of participating electrons. When Larmor precession is present, no more than two electrons may form isotropic spin correlation. In the absence of Larmor spin precession, which is realized by coherent electrons, an arbitrary number of electrons may form isotropic spin correlation.

It follows from our results that the actual particle spin value plays no role and that obeying Fermi–Dirac versus Bose–Einstein statistics is not any inherent property of a particle. Therefore, the categorization of elementary particles into "fermion" versus "boson" classes is not always applicable.

The phenomenology of superconductivity demonstrates that the stability of the delocalized electrons' coherent state is thermodynamically controlled, and thus the realization of Bose–Einstein-condensed electron wavefunctions depends on the thermodynamics of a

given system. Our analysis of coherent electron states demonstrates that they represent a lower entropy of electrons than the Larmor spin precession involving incoherent states. These results facilitate a detailed energy change versus entropy change comparison of possible electron states, which is the pre-condition for a first-principles calculation of the superconducting transition temperature.

As the preference of Fermi–Dirac versus Bose–Einstein statistics is thermodynamically determined for a given system, an increasing mechanical pressure eventually becomes a thermodynamic driver for electron coherence; electron coherence mitigates the growing pressure by allowing for the shared occupancy of low-energy states. The Bose–Einstein condensation of electrons should therefore play a role in astrophysical phenomena that involve extreme gravitational forces and pressures.

Although we focused on electron examples, our equations in fact universally apply to any particle that has a spin. The Bose–Einstein condensation of electrons is observed in the few Kelvin to 100 Kelvin temperature range in superconductors. At ultra-low temperatures, the Bose–Einstein condensation of even $^{87}$Rb nuclei is observed [16], as anticipated. The temperature difference between electron versus $^{87}$Rb condensation relates to the inverse proportionality between the particle mass and its Bose–Einstein condensation temperature.

While the calculation of electron binding energies in the 1920's clarified one half of chemistry, it took 100 years to clarify the other half of chemistry, which is related to electron statistics. We anticipate that our results shall inspire a deeper study of the thermodynamic conditions that determine the applicability of Fermi–Dirac versus Bose–Einstein statistics, and this will lead to the rational design of high-temperature superconductors. Reference [12] represents such a pioneering attempt at exploring the thermodynamics of delocalized electrons' Bose–Einstein condensation.

**Author Contributions:** Conceptualization, A.K. and G.V.; methodology, A.K. and G.V.; validation, A.K. and G.V.; formal analysis, A.K. and G.V.; investigation, A.K. and G.V.; writing—original draft preparation, A.K.; writing—review and editing, A.K.; visualization, A.K. All authors have read and agreed to the published version of the manuscript.

**Funding:** This research received no external funding.

**Data Availability Statement:** No new data were created or analyzed in this study. Data sharing is not applicable to this article.

**Acknowledgments:** The authors thank Jan von Pfaler for clarifications about the London equation's mathematical derivation. The APC was funded by Marc Fleury.

**Conflicts of Interest:** The authors declare no conflicts of interest.

## Appendix A. A Useful Vector Field Identity

Let $\boldsymbol{F}, \boldsymbol{G}$ be vector fields, and let $\Omega$ be a volume region in space. Let $\sigma$ denote the surface of $\Omega$. The field $\boldsymbol{G}$ will serve as a "variation field", and therefore we require it to vanish on the surface of $\Omega$, i.e., $\boldsymbol{G}\,|_{\sigma} = 0$. We start from the following well-known vector field identity:

$$\nabla \cdot (\boldsymbol{F} \times \boldsymbol{G}) = (\nabla \times \boldsymbol{F}) \cdot \boldsymbol{G} - \boldsymbol{F}(\nabla \times \boldsymbol{G})$$

We integrate the above equation over $\Omega$:

$$\int_{\Omega} \nabla \cdot (\boldsymbol{F} \times \boldsymbol{G})\, dV = \int_{\Omega} (\nabla \times \boldsymbol{F}) \cdot \boldsymbol{G}\, dV - \int_{\Omega} \boldsymbol{F}(\nabla \times \boldsymbol{G})\, dV$$

Upon rearranging terms, we obtain

$$\int_{\Omega} \boldsymbol{F}(\nabla \times \boldsymbol{G})\, dV = \int_{\Omega} (\nabla \times \boldsymbol{F}) \cdot \boldsymbol{G}\, dV - \int_{\Omega} \nabla \cdot (\boldsymbol{F} \times \boldsymbol{G})\, dV \tag{A1}$$

We evaluate the last term of the above equation by changing from volume integration to bounding surface integration:

$$\int_{\Omega} \nabla \cdot (\boldsymbol{F} \times \boldsymbol{G})\, dV = \int_{\sigma} \boldsymbol{F} \times \boldsymbol{G}\, dA = 0$$

The above equation evaluates to zero because $\boldsymbol{G}$ vanishes on the surface of $\Omega$. Therefore, Equation (A1) simplifies to

$$\int_{\Omega} \boldsymbol{F}(\nabla \times \boldsymbol{G})\, dV = \int_{\Omega} (\nabla \times \boldsymbol{F}) \cdot \boldsymbol{G}\, dV \tag{A2}$$

## References


1. The Nobel Prize in Physics 2022. Available online: https://www.nobelprize.org/prizes/physics/2022/popular-information/ (accessed on 27 August 2024).
2. Celani, F.; Di Tommaso, A.O.; Vassallo, G. The Electron and Occam's razor. *J. Condens. Matter Nucl. Sci.* **2017**, *25*, 76–99.
3. Schweiger, A.; Jeschke, G. *Principles of Pulse Electron Paramagnetic Resonance*; Oxford University Press: Oxford, UK, 2001.
4. Torizuka, Y.; Hosaka, K.; Schmidt, P.; Odagiri, T.; Knie, A.; Ehresmann, A.; Kougo, R.; Kitajima, M.; Kouchi, N. Entangled pairs of 2p atoms produced in photodissociation of $H_2$ and $D_2$. *Phys. Rev. A* **2019**, *99*, 063426. [CrossRef]
5. O'Hara, P. Rotational invariance and the spin-statistics theorem. *Found. Phys.* **2003**, *33*, 1349–1368. [CrossRef]
6. Kovács, A.; Vassallo, G.; O'hara, P.; Celani, F.; Di Tommaso, A.O. *Unified Field Theory and Occam's Razor: Simple Solutions to Deep Questions*; World Scientific: Singapore, 2022.
7. Hestenes, D. Spin and uncertainty in the interpretation of quantum mechanics. *Am. J. Phys.* **1979**, *47*, 399–415. [CrossRef]
8. Vassallo, G. Charge Clusters, Low Energy Nuclear Reactions and Electron Structure. *J. Condens. Matter Nucl. Sci.* **2024**, *39*. [CrossRef]
9. Jaynes, E.T. Scattering of Light by Free Electrons as a Test of Quantum Theory. In *Chapter 1 in The Electron—New Theory and Experiment*; Springer: Berlin/Heidelberg, Germany, 1991.
10. Hirsch, J.E. BCS theory of superconductivity: It is time to question its validity. *Phys. Scr.* **2009**, 80, 035702. [CrossRef]
11. Uemura, Y.J. Energy-scale considerations of unconventional superconductors—Implications to condensation and pairing. *Phys. C* **2023**, *614*, 1354361. [CrossRef]
12. Kovacs, A.; Vassallo, G. *High-Temperature Superconductivity Is the Catalyzed Bose-Einstein Condensation of Electrons*; KDP: Seattle, WA, USA, 2024.
13. Valla, T.; Drozdov, I.K.; Gu, G.D. Disappearance of superconductivity due to vanishing coupling in the overdoped $Bi_2Sr_2CaCu_2O_{8+d}$. *Nat. Commun.* **2020**, 11, 569. [CrossRef] [PubMed]
14. Bardeen, J.; Cooper, L.N.; Schrieffer, J.R. Theory of Superconductivity. *Phys. Rev.* **1957**, *108*, 1175. [CrossRef]
15. de Gennes, P.G. *Superconductivity of Metals and Alloys*; Perseus Books: New York, NY, USA, 1999.
16. The Nobel Prize in Physics 2001. Available online: https://www.nobelprize.org/prizes/physics/2001/popular-information/ (accessed on 31 August 2024).